Human Amniotic Membrane Enriched with Urinary Bladder Fibroblasts Promote the Re-Epithelization of Urothelial Injury

Urška Dragin Jerman[1], Peter Veranič[1], Tina Cirman[2], and Mateja Erdani Kreft[1] ⑩

Abstract

Culturing cells in three-dimensional systems that include extracellular matrix components and different cell types mimic the native tissue and as such provide much more representative results than conventional two-dimensional cell cultures. In order to develop biomimetic bladder tissue in vitro, we used human amniotic membrane (AM) extracellular matrix as a scaffold for bladder fibroblasts (BFs) and urothelial cells. Our aims were to evaluate the integration of BFs into the AM stroma, to assess the differentiation of the urothelium on BFs-enriched AM scaffolds, and to evaluate the AM as a urothelial wound dressing. First, to achieve the optimal integration of BFs into AM stroma, different intact and de- epithelialized AM (dAM) scaffolds were tested. BFs secreted matrix metalloproteinase (MMP)-1 and MMP-2 and integrated into the stroma of all types of AM scaffolds. Second, to establish urothelial tissue equivalent, urothelial cells were seeded on dAM scaffolds enriched with BFs. The BFs in the stroma of the AM scaffolds promoted (1) the proliferation of urothelial cells, (2) the attachment of urothelial cells on AM basal lamina with hemidesmosomes, and (3) development of multilayered urothelium with expressed uroplakins and well-developed cell junctions. Third, we established an ex vivo model of the injured bladder to evaluate the dAM as a wound dressing for urothelial full-thickness injury. dAM acted as a promising wound dressing since it enabled rapid re-epithelization of urothelial injury and integrated into the bladder tissue. Herein, the developed urothelial tissue equivalents enable further mechanistic studies of bladder epithelial–mesenchymal interactions, and they could be applied as biomimetic models for preclinical testing of newly developed drugs. Moreover, we could hypothesize that AM may be suitable as a dressing of the wound that occurs during transurethral resection of bladder tumor, since it could diminish the possibility of tumor recurrence, by promoting the rapid re-epithelization of the urothelium.

Keywords

Introduction

The human amniotic membrane (AM) is the innermost layer of fetal membranes surrounding the developing fetus. It is normally 0.02–0.5 mm thick and composed of three distinct layers: an epithelial monolayer, basal lamina, and stromal layer. The AM stroma is further divided into a compact layer, a layer of amniotic mesenchymal stromal cells, and a spongy layer[1]. AM has many desired biological properties such as anti-inflammatory[2] and antimicrobial effects[3], anti-fibrotic activity[4,5], low immunogenicity[6], and is at the same time easily obtainable and inexpensive. Therefore, it is often used as a naturally derived biomaterial in tissue engineering and regenerative medicine. Its remarkable regenerative potential has also been demonstrated in the field of urology (reviewed in Ramuta and Kreft[7]), where fresh or cryopreserved AMs were used as a graft for the

---

[1] Institute of Cell Biology, Faculty of Medicine, University of Ljubljana, Ljubljana, Slovenia
[2] Blood Transfusion Centre of Slovenia, Ljubljana, Slovenia

Corresponding Author:
Mateja Erdani Kreft, Institute of Cell Biology, Faculty of Medicine, University of Ljubljana, Vrazov trg 2, SI-1000 Ljubljana, Slovenia.
Email: mateja.erdani@mf.uni-lj.si

reconstruction of the ureter[8], bladder[9,10], or urethra[11]. Although these studies showed the partially reconstructed urinary tract wall, they did not provide any data about the differentiation or functionality of the de novo established urothelia.

The bladder urothelium is a transitional epithelium extending from the renal pelvis to the proximal urethra[12]. It consists of three main types of cells: poorly differentiated basal urothelial cells, partially differentiated intermediate urothelial cells, and highly differentiated superficial urothelial cells, which border the lumen of the urinary bladder and are responsible for maintenance of the blood–urine permeability barrier[13–16]. To date, only a few studies investigated AM as a scaffold for urothelial cell growth and differentiation, and even there with opposite results. The studies used fresh or cryopreserved de-epithelialized AM (dAM) scaffolds, that is, AM deprived of amniotic epithelial cells. Two of them defined dAM as unsuitable for the establishment of the human urothelium[17,18], while the other two reported the formation of mouse and rabbit urothelium-like tissue; however, the differentiation status of urothelial cells was not analyzed[19,20]. In our previous study, we demonstrated that the dAM scaffold promotes the formation of a differentiated porcine urothelium[21].

The scaffolds such as AM that are composed of various extracellular matrix components enable the establishment of three-dimensional (3D) in vitro cell culture models. However, for the even more genuine imitation of the situation in vivo, it is advantageous to improve the model by adding tissue-specific mesenchymal cells. In the urinary bladder, the signaling from the fibroblasts in the lamina propria essentially influences the regeneration of the urothelium as well as contributes to the maintenance of adult differentiation of urothelial cells (reviewed in Jerman et al.[22]). Herein, we investigate the integration of urinary bladder fibroblasts (BFs) into the stroma of AM scaffolds, and we first use the AM as a scaffold for BFs and urothelial cells simultaneously. To the best of our knowledge, only Yang et al.[23] used dAM as a scaffold for fibroblasts and epithelial cells up to now. Using an in vitro skin model, they showed that dAM with integrated skin fibroblasts promotes the establishment of the stratified and well-differentiated epidermis. The established skin equivalent on the dAM scaffold integrated well into the surrounding skin tissue when transplanted onto a full-thickness wound on a nude mouse.

The aims of the present study were: first, to evaluate the integration of urinary BFs into the AM stroma and to assess the differentiation of the urothelium on BFs-enriched AM scaffolds. And the second goal was to evaluate the AM as urothelial wound dressing, by monitoring the regeneration of the native urothelium on AM graft and integration of the native BFs in the AM stroma. For this, we performed (1) in vitro experiments using different AM scaffolds and (2) used dAM as a dressing for full-thickness urothelial injury on the ex vivo model. The characteristics of the obtained urothelial tissue equivalents were evaluated by light microscopy, using various immunofluorescence and histological approaches, and electron microscopy.

Materials and Methods

Cell Cultures

All the experiments using normal porcine urothelial (NPU) cells and urinary BFs were approved by the Veterinary Administration of the Slovenian Ministry of Agriculture and Forestry in compliance with the Animal Health Protection Act and the Instructions for Granting Permits for Animal Experimentation for Scientific Purposes.

Primary and secondary NPU and BFs cultures were established from two porcine urinary bladders, obtained independently from a local abattoir. The exact isolation procedure is described in Zupančič et al. and Jerman et al[24,25]. Briefly, the urinary bladder was removed and cut sagittally into halves. Then each half was cut into 5-cm long and 2-cm wide strips. For isolation of the NPU cells, the urothelium was gently scraped with a scalpel blade. The NPU cells were filtered through a 40-ml Cell Strainer (BD Falcon) and seeded onto polystyrene tissue culture flasks (TPP, Trasadingen, Switzerland) at a density of 2×10^5 viable cells/cm^2. The NPU cells were cultured in medium UroM, which consisted of equal parts of MCDB153 medium (Sigma-Aldrich) and advanced-Dulbecco's modified essential medium (Invitrogen, Life Technologies, Wein, Austria), supplemented with 2.5% fetal bovine serum (FBS; Gibco, Life Technologies), 0.1 mM phosphoethanolamine (Sigma-Aldrich, Taufkirchen, Germany), 15 µg/ml adenine (Sigma-Aldrich), 0.5 µg/ml hydrocortisone (Sigma-Aldrich), 5 µg/ml insulin (Sigma-Aldrich), 4 mM glutamax (Gibco, Life Technologies), and penicillin–streptomycin solution (100 U/ml of penicillin and 100 µg/ml streptomycin; Gibco, Life Technologies, Darmstadt, Germany)[26]. The BFs were isolated from the urinary bladder lamina propria. The lamina propria was separated from the detrusor muscle mechanically using sterile forceps and incubated in collagenase IV (100 U/mL, Sigma-Aldrich) at 37 °C on a shaker for 2 h. The fragments of lamina propria were centrifuged ($200 \times g$; 5 min); the collagenase IV was removed, and BFs were resuspended in culture medium adapted for BFs (BFM) and seeded onto polystyrene tissue culture flasks (TPP) at a density of 5×10^4 viable cells/cm^2 The BFM medium contained advanced-Dulbecco's modified essential medium (Invitrogen, Life Technologies), supplemented with 10% FBS (Gibco, Life Technologies, Darmstadt, Germany), 4 mM glutamax (Gibco, Life Technologies), and penicillin–streptomycin solution (100 U/ml of penicillin and 100 µg/ml of streptomycin; Gibco, Life Technologies). For secondary cell cultures, the primary NPU as well as BFs cultures at 80% confluency were incubated in TrypLE Select (Gibco) at 37 °C for 10–20 min. The de-attached cells were collected, centrifuged, and replated on fresh tissue culture flasks. The secondary cultures of NPU cells of V–VII passages and BFs of II–

XV passages were cultured at 37 °C in a 95% humidified atmosphere with 5% carbon dioxide. The UroM and BFM media were changed three times a week on alternate days.

The identity of the isolated NPU cells and BFs was confirmed by immunolabeling of uroplakins, cytokeratin 7, vimentin, and desmin as described in Zupančič et al[24].

Preparation of the AM

The use of the human AM was approved by the National Medical Ethics Committee of the Republic of Slovenia. Placentas were obtained according to the local regulations and with written informed consent at the time of elective cesarean sections from overall healthy donors. All the donors were additionally tested for human immunodeficiency virus (HIV), syphilis, and hepatitis B and C, and were serologically negative.

The placenta was aseptically washed with phosphate-buffered saline (PBS) containing 50 mg/ml penicillin, 50 mg/ml streptomycin, 100 mg/ml neomycin, and 2.5 mg/ml amphotericin B. The AM was manually separated from the chorion; AM was then placed on the nitrocellulose membrane, cut into pieces of 4 × 4 cm^2, and cryopreserved at −80 °C in the Eagle's medium and glycerol in a volume ratio of 1:1 for not more than 24 months. The possible infection of a donor with HIV, syphilis, and hepatitis B and C had been excluded by serological tests according to the local regulations. Before the use, frozen AMs were thawed, washed with sterile PBS or medium BFM, and anchored into membrane holders of 14 mm in diameter (CellCrown, Scafdex, Finland), with the epithelial side facing upward or downward. Altogether, the experiments were performed using the AMs from 10 donors.

To obtain the dAM, two different methods were used. To acquire the dAM scaffold composed of basal lamina and stroma, we used thermolysin, diluted in PBS (1:50; Sigma-Aldrich). The thermolysin was added to the epithelial side of the AM scaffold for 15 min at 37 °C. After the incubation, the AMs were immediately rinsed and washed twice for 15 min in PBS to remove cellular debris. To obtain the dAM scaffold composed of only AM stroma, we used dispase I diluted in BFM medium (1.6 mg/ml, Roche, Germany). The dispase I was added to the epithelial side of the AM scaffold and incubated for 45 min at 37 °C. After the incubation, the AMs were immediately washed three times in the BFM medium.

Establishment of BFs-Enriched AM Scaffold

To evaluate the integration of BFs into the stroma of intact AM or dAM, the BFs (V–XV passage) were seeded onto six-well culture inserts with porous membranes with 0.4 μm pores and 4.2 cm^2 effective growth area (BD Falcon). The seeding density was 1 × 10^5 cells/cm^2. After the BFs reached subconfluency, they were labeled using green fluorescent lipophilic dye (1:200; Vybrant DiO, ThermoFisher

Scientific, Taufkirchen, Germany). The AMs, anchored into the membrane holders, were placed onto the labeled BFs in a way that the BFs were in contact with: (1) epithelium or spongy layer of intact AM; (2) compact layer, basal lamina, or spongy layer of dAM. BFs were cultured with AM, in the BFM medium, for 1–3 weeks. For each of the AM scaffolds, we conducted at least three independent experiments.

Establishment of the Urothelial Tissue Equivalent

To establish the urothelial tissue equivalent, we used dAM scaffolds with BFs integrated into the AM spongy layer. To populate the dAM spongy layer, the BFs were cultured in contact with the AM spongy layer in the BFM medium for 1 week (dAM [BFs/SL]; Fig. 1). Afterward, the NPU cells (V–VII passage) were either seeded onto the basal lamina of the BFs-enriched dAM scaffolds at the seeding density of 2 × 10^5 cells/cm^2 or onto the basal lamina of dAM scaffolds without the integrated BFs (Fig. 1). Before the seeding of NPU cells, the AM scaffolds were kept in the BFM medium for a week. At the time of the seeding of NPU cells, the growth medium was changed from the BFM to the UroM medium. The provided culture conditions were optimal for the growth of the NPU cells. In the UroM medium, the BFs remains viable; however, their proliferation rate significantly decreases[24]. In our situation, this was appreciated, since it prevented BFs to expand excessively. NPU cells were maintained in the culture for an additional 3 weeks and were regularly examined with an inverted microscope Leica DM IL (Leica Microsystems). For each of the dAM scaffolds, we performed at least three independent experiment replications in triplicates.

Establishment of the Ex Vivo Model of Injured Bladder and Application of the dAM as a Wound Dressing

To establish an ex vivo model of the injured bladder, the porcine urinary bladder was cut sagittally into halves. The sections of the bladder tissue with the area of approximately 2 cm^2 were cut from the region above the bladder trigonum. In the cross-section, the excised bladder tissue included the urothelium, lamina propria, and detrusor muscle of approximately 1 cm of the total thickness. In order to ensure a sufficient flow of nutrients to the entire bladder tissue, the detrusor muscle of approximately 0.5 cm thickness was removed. In each segment of the excised bladder tissue, we made a full-thickness urothelial injury of approximately 25 mm^2, which included the urothelium and the upper half of the lamina propria in the cross-section. The segments of the bladder tissue with full-thickness urothelial injuries were washed with fresh UroM medium and placed on six-well culture inserts with porous membranes with 0.4 μm pores and 4.2 cm^2 effective growth areas (BD Falcon). The bladder tissue was positioned at the air–liquid interface. The dAM graft with the basal lamina positioned upward was applied to the site of the full-thickness urothelial injury using fibrin
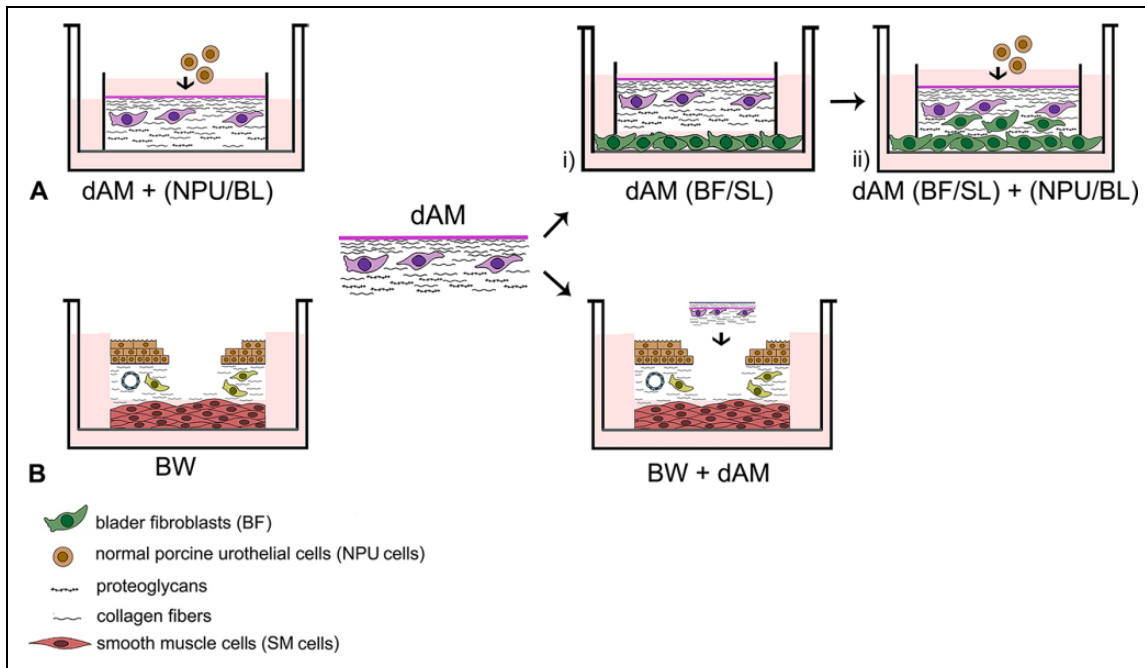
Fig. 1. Schematic representation of the experiment design. Experiments were performed with the dAM scaffolds that were previously treated with thermolysin. (A) Establishment of the urothelial tissue equivalent. dAM scaffolds without BFs served as a control (dAM + (NPU/BL)). (1) BFs were cultured in contact with the SL of the dAM scaffolds (dAM (BFs/SL)). (2) NPU cells were seeded onto the (BL) of the BFs-enriched dAM scaffolds (dAM (BFs/SL) + (NPU/BL)). (B) Evaluation of the dAM graft for urothelial regeneration. The models without applied dAM were used as controls (BW). The dAM graft was applied to the ex vivo model of urothelial full-thickness injury (BW + dAM). AM: amniotic membrane; BFs: bladder fibroblasts; BL: basal lamina; BW: bladder wall; dAM: de-epithelialized AM; NPU: normal porcine urothelial; SL: spongy layer.

glue (Beriplast P Combi-set, CSL Behring). The full-thickness urothelial injuries without applied dAM served as controls (Fig. 1). The models were cultured in the UroM medium for a week. To remove cell debris, the models were rinsed with the UroM medium every day, and the UroM medium was replaced with the fresh one. The experiment was performed using the bladder tissue isolated from a single urinary bladder. We conducted one independent experiment with three technical repeats.

Analysis of NPU Cell Growth on dAM Scaffolds

To evaluate the growth of the NPU cells on the dAM scaffolds, the NPU cells were inspected with a transmitted light inverted microscope Eclipse TE300 (Nikon). The first and the third day after the NPU cell seeding, we took the images of 1.15 mm^2 of the NPU cell culture. The sites of the imaging were selected randomly. The images were analyzed using Image J software. The areas of the dAM scaffold covered with the NPU cells were outlined by the selection tool, and the area of these regions was measured. We analyzed 73 images of NPU on dAM and 71 images of NPU on BFs-enriched dAM scaffolds, all from four independent experiments.

Histological and Immunofluorescence Analyses

The AM scaffolds with integrated BFs, the urothelial tissue equivalents on dAM scaffolds/grafts were fixed in 4% paraformaldehyde in PBS for histological staining or immunofluorescence labeling. For histological staining, the samples were dehydrated through a graded series of ethanol into xylene and embedded in paraffin wax. Once dewaxed, the 5 µm paraffin sections were stained with hematoxylin–eosin (Sigma-Aldrich). For the immunofluorescence, the samples were embedded in the Jung tissue freezing medium (Leica), frozen and cut into 7 µm frozen sections. After air-drying and washing in PBS, the sections were blocked in 1% bovine serum albumin (BSA) in PBS at room temperature for 1 h and incubated at 4 °C overnight with primary antibodies as follows: rabbit polyclonal antibodies against uroplakins (1:1000; a gift from Professor T.T. Sun), rabbit polyclonal antibodies against type IV collagen (1:400; Abcam), and mouse monoclonal antibodies against integrin β4 (1:100; Abcam), all diluted in 1% BSA in PBS. After washing in PBS, sections were incubated with appropriate secondary antibodies: goat antimouse (1:400; Alexa Fluor 555; Invitrogen, Molecular Probes) or goat antirabbit (1:400; Alexa Fluor 555; Invitrogen, Molecular Probes), at room temperature for 1 h. After washing in PBS, the samples were mounted in Vectashield mounting medium with 4′,6-

diamidino-2-phenylindole (DAPI) (Vector Laboratories, Burlingame, CA) for DNA labeling. We performed negative controls by omitting primary antibodies or the use of irrelevant primary antibodies. The samples were analyzed using a fluorescence microscope Eclipse TE300 (Nikon) or Labor-LuxS (Leitz).

Analysis of the Urothelial Stratification

The stratification of the urothelia on the dAM scaffolds with or without integrated BFs was determined by counting the cell nuclei of the established urothelia. The analysis was based on the assumption that the urothelial cell possesses one nucleus. To label the nuclei, randomly selected frozen sections of the urothelia on the dAM scaffolds with or without integrated BFs were mounted in Vectashield mounting medium with DAPI (Vector Laboratories) to stain the nuclei blue. The nuclei were counted on the 2 mm long segments ($N = 7$ for dAM scaffolds and $N = 5$ for BFs-enriched dAM scaffolds) of the urothelia using the Cell Counter plugin of the ImageJ software.

Gelatin Zymography

Gelatin zymography was used to detect the matrix metalloproteinases (MMPs), secreted by BFs cultured in contact with the dAM scaffold in BFM growth medium, supplemented with FBS. To detect the gelatinolytic bands resulting from the MMPs present in the FBS, we included the additional controls: (1) 100% FBS and (2) BFM growth media with or without supplemented FBS. In the latter case, the BFs were cultured on the porous membranes. To exclude the possible MMPs from the AM scaffold itself, the growth media incubated with the dAM scaffold alone were also analyzed. The growth media were collected from the BFs on the first, third, and seventh day of cultivation, taking into account that the media were replaced with fresh ones 24 h before the harvest. The collected growth media were centrifuged (10 min, 200 × g, 4°C), and the supernatants were frozen at −80°C. The protein concentration in the samples was determined by the bicinchoninic acid assay method. The samples with a final concentration of 5 μg proteins/μl were separated using 10% sodium dodecyl-polyacrylamide electrophoresis on gels containing 0.1% gelatin at 4°C. Afterward, the gels were rinsed in distilled water and incubated in the renaturation protein buffer (2.5% Triton X-100 in distilled water) with gentle agitation, twice in 60 min. After that, the gels were rinsed once more with distilled water and incubated for 42 h at 37 °C in the developing buffer (0.5 M Tris hydrochloric acid (pH 7.8), 2 M sodium chloride, 0.05 M calcium chloride, 0.2% Triton X-100 in distilled water). The gels were stained with Coomassie blue (Bio-Rad, 0.5% Coomassie blue, 5% methanol, 10% acetic acid in distilled water) for 1 h and destained in destaining solution (5% ethanol, 10% acetic acid in distilled water). The MMP activity in the gel was identified as white bands against a blue background. We analyzed samples from two independent experiments.

Transmission and Scanning Electron Microscopy

For transmission electron microscopy, the AM scaffolds, the AM scaffolds with integrated BFs, and the urothelial tissue equivalents on dAM scaffolds were fixed in 3% (w/v) paraformaldehyde and 3% (v/v) glutaraldehyde in a 0.1 M cacodylate buffer, pH 7.4 for 3 h at 4 °C. The ex vivo models of full-thickness urothelial injury with or without dAM grafts were fixed in the same fixative, but overnight at 4 °C. The fixation was followed by overnight rinsing in the 0.1 M cacodylate buffer at 4 °C and a postfixation in 2% (w/v) osmium tetroxide for 1 h at room temperature. The samples were then dehydrated in a graded series of ethanol and embedded in Epon (Serva Electrophoresis, Heidelberg, Germany). In the case of the ex vivo models of the injured bladder, the ethanol dehydration was followed by dehydration in propylene oxide. The samples were next embedded in a mixture of propylene oxide and Epon (1:1) overnight at 4 °C and then embedded in Epon. Ultrathin sections were contrasted with uranyl acetate and lead citrate and examined with a transmission electron microscope (Philips CM100).

For scanning electron microscopy, the AM scaffolds and the urothelial tissue equivalents on dAM scaffolds were fixed in 2% (w/v) paraformaldehyde and 2% (v/v) glutaraldehyde in a 0.2 M cacodylate buffer, pH 7.4 for 3 h at 4 °C. The ex vivo models of full-thickness urothelial injury with or without dAM grafts were fixed in the same fixative, but overnight at 4 °C. The samples were rinsed in 0.2 M cacodylate buffer overnight at 4 °C and postfixed in 1% osmium tetroxide in the same buffer for 2 h at room temperature. After rinsing in 0.2 M cacodylate buffer and dehydration in a graded series of ethanol, the samples were completely dehydrated in acetone and hexamethyldisilazane (Sigma-Aldrich). The samples of the ex vivo models of the injured bladder were dried at the critical point (Baltec CPD 030). The dehydrated samples were sputtured with gold and examined with a scanning electron microscope (Tescan Vega 3).

Analysis of the Urothelial Differentiation

The analysis of the urothelial differentiation on the dAM scaffolds with or without integrated BFs was performed on scanning electron micrographs using the ImageJ software. The sites of the imaging were selected randomly. In each scanning electron micrography, we outlined the NPU cells with apical plasma membrane shaped into microvilli as opposed to the NPU cells with ropy or rounded ridges on the apical surface. We analyzed 30 micrographs of NPU cells on dAM and 30 micrographs of NPU cells on BFs-enriched dAM scaffolds. Samples were obtained from two independent experiments.

Statistical Analysis

Presented data are expressed as mean $\pm$ standard error. A statistically significant difference between dAM scaffolds

covered with the NPU cells was tested by *F*-test and two-sided Student's *t*-test. *P*-values of <0.05 were considered statistically significant. For each experiment, the number of independent experiments and the analyzed images/regions is stated in the figure legends.

Results

BFs Secrete MMP-1 and MMP-2 and Most Successfully Integrate into the AM Spongy Layer

Histochemical and histological analyses have shown that BFs integrated most successfully into the spongy layer of the intact AM or dAM (Fig. 2A–D). They populated the spongy layer in just 1 week (Fig. 2C, D). The BFs incorporated well into the dAM compact layer as well (Fig. 2E, F). BFs crossing of AM basal lamina was observed rarely and predominantly in models, where AM was treated with thermolysin (Fig. 2G-J). Overall, the BFs were the least successful in crossing the basal lamina of intact AM since they first had to penetrate the amniotic epithelial cell (AEC) monolayer (Fig. 2G, H). The BFs grown in contact with the AM scaffolds secreted type IV collagen. However, the only situation in which we could conclude this with certainty was when BFs were cultured in contact with AM epithelium or AM basal lamina (Fig. 2 H, J). In these cases, the BFs were positioned on the opposite side of the AM stroma, and the signal of type IV collagen labeling around the BFs could not belong to the AM scaffold itself.

The ultrastructural analysis confirmed that the BFs remained viable after integration in the AM spongy layer (Fig. 3A). Their viability was confirmed also when they were cultured in the UroM medium (data not shown). Using the gelatine zymography, we detected the MMP-1 and MMP-2 in the BFM (supplemented with 10% FBS) collected from the BFs cultured in contact with the dAM scaffolds (Fig. 3B). The MMP bands were the most pronounced on the seventh day of cultivation, which is most probably due to an increased number of BFs in the culture. We also detected the MMPs in the media of BFs cultured on the porous membranes. However, the detection of MMP-2 was reduced when we cultured BFs on the porous membranes in the BFM without adding FBS. This suggests that BFs in the cell culture require FBS-supplemented growth medium to secret the MMPs and to integrate into the AM stroma. These data were additionally confirmed by hindered integration of the BFs into the AM stroma when they were cultured in UroM supplemented with only 2.5% FBS (data not shown).

BFs in the AM Stroma Promote the Attachment of NPU Cells to the dAM Basal Lamina and Stimulate Their Proliferation

We evaluated the attachment and growth of NPU cells on the basal lamina of dAM scaffolds and BFs-enriched dAM scaffolds on the first and third days after the NPU cell seeding.

One day after the seeding, the NPU cells covered $44.8\% \pm 2.5\%$ of the dAM scaffolds and $58.4\% \pm 2.7\%$ of the BFs-enriched dAM scaffolds, $P < 0.001$ (**Fig. 4**A–C). After 3 days in culture, the difference between the coverage of the dAM scaffolds with the NPU cells was no longer significant since the NPU cells covered $90.4 \pm 2.8\%$ of the dAM scaffolds and $92.9\% \pm 1.7\%$ of the BFs-enriched dAM scaffolds (Fig. 4C). The histological analysis of the established urothelia after 3 weeks in culture demonstrated that when seeded on the dAM scaffold, NPU cells formed two-layered to three-layered urothelium, while the urothelium on the BFs-enriched dAM scaffolds consisted of 3–4 cell layers (Fig. 4D–F). The difference in the stratification of the urothelia on the dAM and BFs-enriched dAM scaffolds was also confirmed by the enumeration of the nuclei of the established urothelia. Overall, we counted 109 ± 9 nuclei in the 2 mm long segments of the urothelia on the dAM scaffolds, and 167 ± 23 cell nuclei in the urothelia of the same length on the BFs-enriched dAM scaffolds, $P \leq 0.05$ (Fig. 4F).

BFs Promote the Development of a Multilayered Uroplakin-Expressing Urothelium

During the process of the differentiation, urothelial cells acquire unique molecular and ultrastructural characteristics that allow the assessment of their differentiation stage and functionality. Among the most recognizable morphological characteristics of the differentiated cells are (1) uroplakin expression in the apical plasma membrane, (2) apical plasma membrane shaped into concave-looking urothelial plaques as seen on transmission electron micrographs or in rounded and microridges as recognized on scanning electron micrographs, (3) uroplakin-transporting discoidal or fusiform vesicles in the apical cytoplasm, and (4) well-developed tight junctions[27]. Herein we have shown that after 3 weeks in culture, NPU cells reached a higher stage of differentiation on dAM scaffolds alone when compared with BFs-enriched dAM scaffolds ($P < 0.005$) (**Fig. 5**). The superficial NPU cells of the urothelia established on dAM scaffolds expressed uroplakins in the apical plasma membrane (Fig. 5A). Moreover, among the superficial urothelial cells with microvilli on the apical surface, there were differentiated superficial cells with apical plasma membrane shaped in characteristic urothelial plaques of concave appearance and rounded ridges ($10.9 \pm 2.9\%$) (Fig. 5C, E). On the other hand, the superficial NPU cells of the urothelia established on BFs-enriched dAM scaffolds achieved a lower differentiation stage. Although they expressed uroplakins in the apical plasma membrane and apical cytoplasm (Fig. 4B), the ultrastructural analysis demonstrated that the vast majority ($99 \pm 1.3\%$) of superficial NPU cells had microvilli on the apical surface (Fig. 5D, F). On both dAM scaffolds, the adjacent superficial urothelial cells were interconnected by tight junctions (Fig. 5C′, D′).

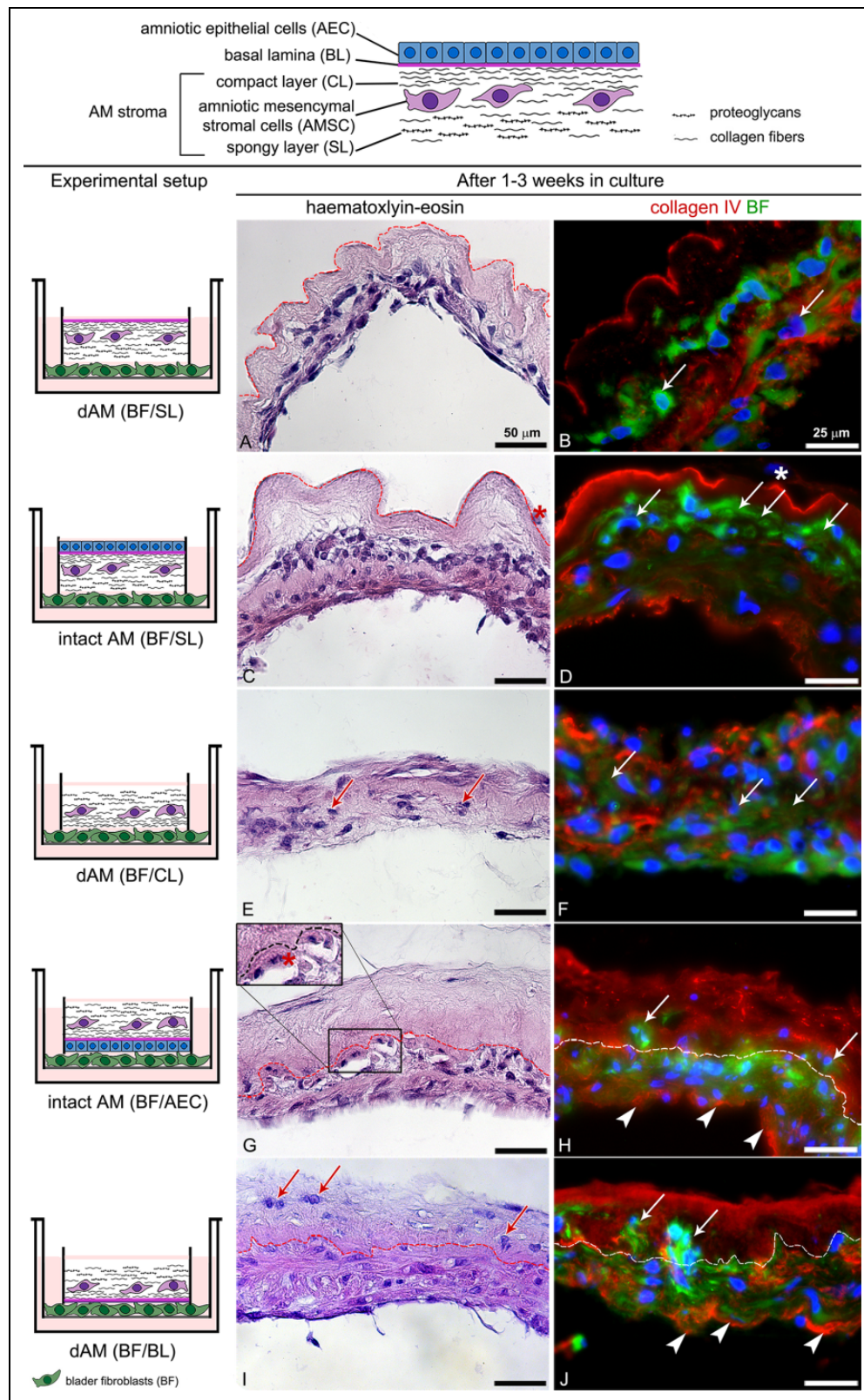The immunolabeling showed that basal NPU cells of the urothelia established on both types of scaffolds expressed

Fig. 2. Histological and histochemical data showing the ability of BFs integration into different AM scaffolds. The BFs were cultured in contact with a spongy layer (BFs/SL) (A–D), compact layer (BFs/CL) (E, F), amniotic epithelial cells (BFs/AEC), (G, H) and basal lamina (BFs/BL) (I, J) for 1 (A, B) or 3 weeks (C–J) in culture. (A–D) BFs (arrows) successfully integrates into the AM spongy layer (SL). In 1 week, they populate the AM spongy layer (A, B) and within 3 weeks they expand to the AM compact layer (C, D). After 3 weeks in culture, AECs gradually exfoliate and only individual AECs can be found (asterisks on C and D). (E, F) The BFs (arrows) infiltrates into the dAM compact layer and in 3 weeks populate the whole scaffold. (G–J) After 3 weeks in culture, the BFs less frequently cross the AM (basal lamina and integrate into the underlying compact layer (arrows in H–J). The BFs grown in contact with AM synthesize type IV collagen (arrowheads in H, J). Dashed lines indicate the AM basal lamina. The large insert on G represents an image of the corresponding smaller insert, enlarged by 50%. DNA is stained blue. BF are stained green with DiO lipophilic dye.
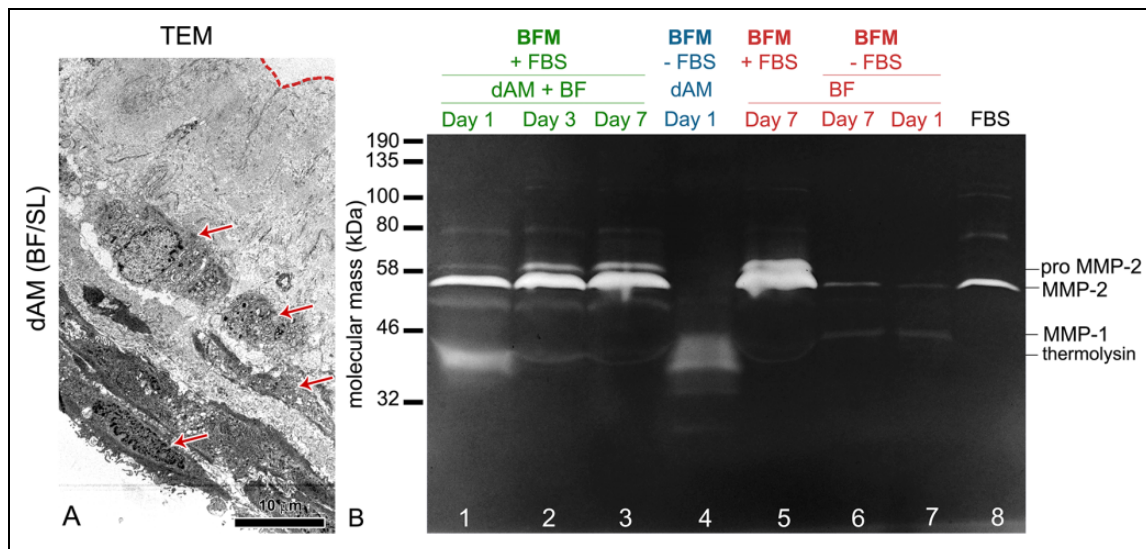
Fig. 3. Integration of bladder fibroblasts (BFs) in the de-epithelialized amniotic membrane (dAM) spongy layer. (A) The ultrastructural analysis shows viable BFs (arrows) integrated into the AM spongy layer after 1 week in growth medium adapted for fibroblasts (BFM). The dashed line indicates the AM basal lamina. (B) The gelatine zymogram analysis. Gelatinolytic activity of (1) BFs cultured in contact with the dAM spongy layer (dAM (BFs/SL); lines 1–3), (2) dAM alone (line 4), and (3) BFs cultured on porous membranes (lines 5–7) on the first, third, and seventh day of cultivation. Proteolytic activity is visualized as white bands on dark background. The detected bands represent proform and the active form of matrix metalloproteinases (MMP)-2 and active form of MMP-1. In 1 week, the gelatinolytic bands of the media from the cultures of BFs grown in contact with dAM become more pronounced (lines 1–3). The MMPs are also detected in the media of the BFs cultured on the porous membranes (lines 5–7). Note the reduced detection of MMP-2 in the media of BFs cultured without fetal bovine serum (FBS; lines 6 and 7). The MMPs detected in 100% FBS are shown in line 8. The gelatinolytic band at 37 kDa represents thermolysin, a protease which was used to remove amniotic epithelial cells. The detection of the thermolysin is pronounced on the first day of the cultivation in the samples of dAM (BFs/SL) (line 1) and dAM (line 4). During the media changes, the thermolysin is gradually washed out and after a week in culture, it is not detectable anymore. Molecular weights of proteases: MMP-2: 58 kDa, proMMP-2: 72 kDa, MMP-1: 43 kDa, thermolysin: 37 kDa.

integrin β4 in the plasma membrane (Fig. 5G, H). However, the ultrastructural analysis revealed that basal NPU cells of urothelia on the BFs-enriched dAM scaffolds form more hemidesmosomes than those of urothelia established on dAM scaffolds alone (Fig. 5I, J).

dAM as Wound Dressing Promotes Regeneration and Development of Differentiated Urothelium

To evaluate the integration of the native BFs into the AM stroma and regeneration of the native urothelium on the dAM, we applied dAM with the basal lamina facing upward to the ex vivo model of a full-thickness urothelial injury (Fig. 6A). After a week in culture, dAM grafts remained at the site of the application. Urothelial cells from the native urothelium overgrew the entire basal lamina of the dAM graft and in a week established two-layered to three-layered urothelium (Fig. 6B). The native BFs from the lamina propria integrated into the dAM spongy layer (Fig. 6C). Superficial urothelial cells of the new urothelium displayed apical plasma membrane shaped into rounded ridges and urothelial plaques of concave appearance (Fig. 6E, G). Among them were partially differentiated superficial urothelial cells that had apical plasma membrane shaped into microvilli (Fig.

6G). Superficial cells were interconnected by tight junctions (Fig. 6D′, E′). Basal urothelial cells were attached to the dAM basal lamina with hemidesmosomes (Fig. 6I), similar as they are in the urothelium in vivo (Fig. 6 H).

Discussion

In the present study, we showed that AM extracellular matrix enables rapid resealing of urothelial injury and development of urothelial tissue equivalent. The approaches used to develop a biomimetic urothelium in vitro can vary greatly from one another (reviewed in Baker et al.[16]). The variables that could affect the success of the establishment of the urothelium in vitro include (1) the culture system of urothelial cells used (e.g., explant cultures, primary cultures, or even immortalized cell cultures), (2) the scaffolds used for cell culture, and (3) the culture conditions (e.g., co-culture with other types of cells, conditioned medium). Generally, the urothelial cell monocultures are still the most frequently used urothelial in vitro model; nevertheless, a lot of research is being done to develop urothelial models that mimic the native situation in the bladder as far as possible. One such approach was described by Bouhout et al.[28] who established the urinary
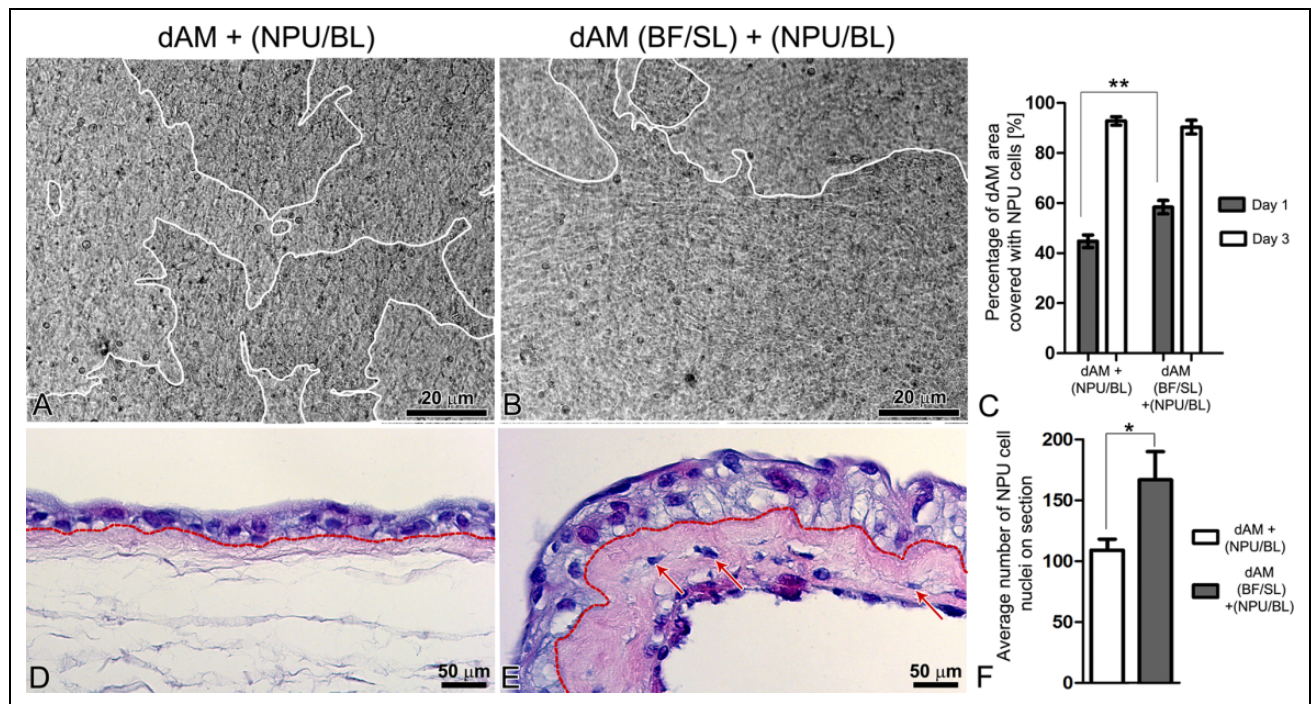
Fig. 4. Analysis of normal porcine urothelial (NPU) cell growth and histological structure of the established urothelia. (A–C) After seeding for 24 h, the NPU cells cover a significantly larger area of the bladder fibroblast (BFs)-enriched de-epithelialized amniotic membrane (dAM) scaffolds (B) when compared with the dAM scaffolds alone (A); $P < 0.001$ (C). The white lines on A and B surround area of the dAM, overgrown with the NPU cells. On the third day of cultivation, the difference in the areas covered by the NPU cells, seeded on two different scaffolds is no longer significant; $P > 0.05$ (C). (D, E) After 3 weeks in culture, the NPU cells on the dAM scaffolds form two-layered to three-layered urothelium (D), whereas urothelia established on the BFs-enriched dAM scaffolds consist of 3–4 layers of NPU cells (E). Dashed lines indicate the AM basal lamina. (F) The significant difference in the stratification of the urothelia between the scaffolds is confirmed by counting the nuclei of the established urothelia; $P < 0.05$. (C) The graph presents the mean percentage of the dAM scaffolds covered with the NPU cells ($N = 73$ analyzed images of NPU cells on dAM scaffolds and $N = 71$ analyzed images of NPU cells on BFs-enriched dAM scaffolds, all from four independent experiments). (F) The average number of the NPU cell nuclei on the 7 μm thick and 2 mm long segments of the urothelium ($N = 7$ segments of the urothelium for dAM scaffold and $N = 5$ segments of the urothelium for BFs-enriched dAM scaffolds, from two independent experiments) $\pm$ SE * $P \leq 0.05$, ** $P < 0.001$.

bladder model by exposing urothelial cells to urine. Such an approach could also be relevant for further optimization of the models described herein. Since the extracellular matrix components are known to affect cellular behavior, the culturing of cells in 3D systems that mimic key factors of tissue is a much more representative of the in vivo environment than simple 2D monolayers (reviewed in Langhans[29]). Moreover, the fibroblasts have a significant impact on the proliferation and differentiation of the epithelial cells[22] and may thus represent an important component of the biomimetic in vitro models. Herein, we show the faster establishment of stratified urothelium on the dAM matrix enriched with BFs, as well as faster re-epithelization of the urothelial injury by using the dAM matrix enriched by native BFs.

In order to achieve the optimal integration of BFs into the AM stroma, we first tested different intact or dAM scaffolds. Our results demonstrate that the most rapid and efficient integration of BFs into the AM stroma occurs when BFs are cultured in contact with the spongy layer of either intact or dAM. These data are in agreement with Yang et al.[23] who demonstrated that skin fibroblasts can integrate into the dAM spongy layer. By gelatine zymography, we detected the gelatinolytic bands that correspond to the MMP-1, MMP-2, and its proform in the growth medium of BFs cultured in contact with the dAM scaffolds. Both MMPs are able to degrade collagens of types I–V, type VII collagen, laminin, and fibronectin[30], which are all components of the AM extracellular matrix[31]. The secretion of MMPs and consequent rearrangement of the AM extracellular matrix might enable BFs to integrate into the spongy layer of AM. The BFs, grown in contact with AM scaffolds, secreted type IV collagen and by surrounding themselves with collagen fibers, they were additionally integrated into the AM scaffolds. Altogether, BFs adhered to all types of AM scaffolds and eventually integrated them into the stromal matrix. This indicates that the orientation of the AM scaffold does not have a crucial role in the integration of BFs into AM stroma and that it would also probably not affect the integration of the AM graft into the surrounding bladder tissue. This is an
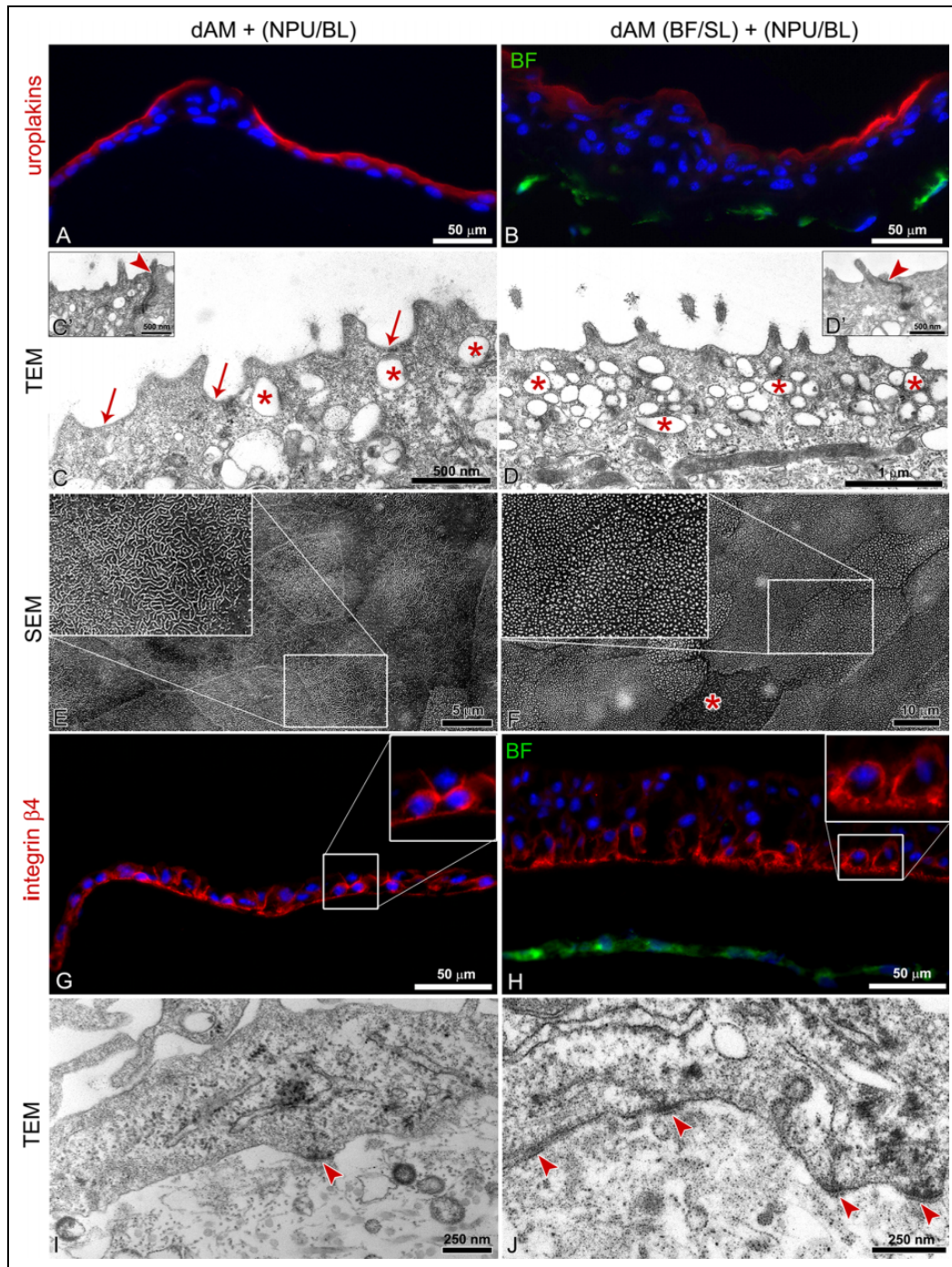
Fig. 5. Histochemical and ultrastructural analysis of the established urothelia after 3 weeks in culture. (A, C, E) The superficial urothelial cells on the de-epithelialized amniotic membrane (dAM) scaffolds express uroplakins in the apical plasma membrane (A). The apical plasma membrane of differentiated superficial cells is shaped in concave-shaped urothelial plaques (arrows on C) and ropy and rounded ridges (E). Shown are the most differentiated superficial urothelial cells. (B, D, F) The superficial urothelial cells on the bladder fibroblasts (BF)-enriched dAM scaffolds display the lower expression of uroplakins in the apical plasma membrane. Their apical plasma membrane is predominantly shaped into microvilli (D, F), although individual cells display ropy ridges (asterisk in F). On both scaffolds, superficial urothelial cells possess numerous discoidal or fusiform-shaped vesicles (asterisks) in the apical cytoplasm (C, D) and tightly interconnect (arrowheads in C′, D′ mark tight junctions). (G, H) Basal normal porcine urothelial (NPU) cells express integrin β4 in the plasma membranes, irrespective of whether they are grown on basal lamina of dAM scaffolds or BFs-enriched dAM scaffolds. (I, J) Ultrastructural analysis of the NPU cells demonstrated that basal NPU cells attach to the basal lamina with more hemidesmosomes when cultured on the BFs-enriched dAM scaffolds rather than on dAM scaffold alone (arrowheads). The large inserts on E–H represent corresponding smaller inserts, enlarged by 100%. DNA is stained blue. BFs are stained green with DiO lipophilic dye.
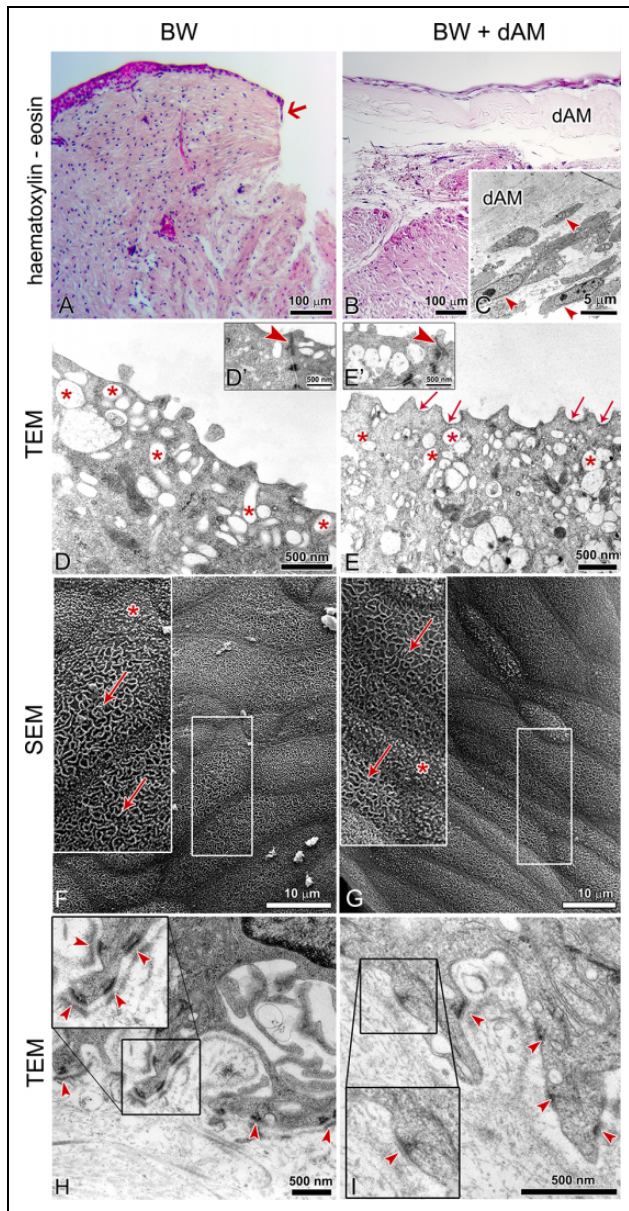
Fig. 6. De-epithelialized amniotic membrane (dAM) as a wound dressing for urothelial full-thickness injury. The samples were analyzed after a week in culture. (A) The non-treated, full-thickness injury of the urothelium does not regenerate within a week in culture. The arrow in A points to the beginning of the urothelial cell growth. (B) Urothelial cells that migrated from the native urothelium surrounding the injury form the two-layered to three-layered urothelium on the basal lamina of the dAM graft. Bladder fibroblasts from the native lamina propria integrate into the spongy layer of the grafted dAM (arrowheads in C). (D, F) After a week in culture, the majority of the superficial urothelial cells of the native urothelium remain differentiated, with apical plasma membrane shaped into rounded ridges (arrows in F). Among them are partially differentiated cells with the apical plasma membrane shaped in microvilli (D, asterisk on F). (E, G) The differentiated superficial urothelial cells on dAM graft have apical plasma membrane shaped in concave-shaped urothelial plaques (arrows in E) and rounded ridges (arrow in G). Shown are the most *(to be Continued.)*

important result, as it suggests the convenience of the AM wound dressing application in clinical urology in the future.

In the second part of the study, we characterized the urothelial tissue equivalents established on the BFs-enriched dAM scaffolds. We demonstrated that BFs in the dAM stroma promote attachment of the NPU cells to the dAM basal lamina and the establishment of a multilayered urothelium, firmly attached to the dAM scaffold by hemidesmosomes. Fibroblasts promote attachment of epithelial cells through the secretion of extracellular matrix[32] or by paracrine signaling[33]. In our case, the BFs and the NPU cells were physically separated by AM basal lamina matrix. Thus, the NPU cells were not in direct contact with the BFs or with the BFs-conditioned medium. We assume that BFs affected the attachment of the NPU cells by secretion of chemotactic paracrine factors that reached the NPU cells by diffusion through the AM extracellular matrix.

The examination of the live NPU cell cultures with a transmitted light inverted microscope showed that after 3 days in culture, the NPU cells covered almost whole basal lamina of the dAM scaffolds, regardless of the presence of the BFs. Nevertheless, the histological analysis of the urothelia established on the dAM and BFs-enriched dAM scaffolds after 3 weeks in culture demonstrated that urothelia on BFs-enriched dAM scaffolds were significantly more stratified. This suggests that the BFs promote the proliferation of the NPU cells and stratification of urothelia.

After 3 weeks in culture, the superficial NPU cells reached the highest degree of differentiation when cultured on the basal lamina of the dAM scaffolds. These results are consistent with the results of our previous study[21] and confirm the dAM basal lamina as a suitable matrix for the establishment of the differentiated urothelium. The differentiation of the superficial NPU cells on the BFs-enriched dAM scaffolds was lower, even though the cells were likewise cultured on the AM basal lamina. Since in vivo porcine urothelium is up to five-layered, we presume that continuous paracrine signaling from the BFs primarily directed the NPU cells toward proliferation, in order to reach the proper stratification. Prolonged culturing of the urothelial equivalents in vitro could thus lead to a more

Fig. 6. (Continued). differentiated superficial urothelial cells. Among them are superficial cells with apical plasma shaped in microvilli (asterisk in G). Superficial cells of both, the native urothelium and the urothelium on the dAM graft, contain a number of discoidal or fusiform-shaped vesicles in the apical cytoplasm (asterisks in D, E) and they interconnected by tight junctions (arrowheads on D', E'). (H, I) The basal urothelial cells on the dAM graft have basal part of plasma membrane shaped into the protrusions (I) and attach to the dAM basal lamina by hemidesmosomes (arrowheads), which is similar to the native urothelium (H, arrowheads mark hemidesmosomes). The large inserts on E–I represent corresponding smaller inserts, enlarged by 100% (E–G) or 50% (I, J). BW: bladder wall.

differentiated urothelium, although, further studies would be required to confirm this hypothesis.

The AM basal lamina is a favorable substrate for the formation of new hemidesmosomes[23] since it is abundant with type VII collagen[34]. We have confirmed the adequacy of AM basal lamina matrix for hemidesmosome formation in vitro and demonstrated that BFs promote firm attachment of the urothelia to the dAM basal lamina via hemidesmosomes. This was additionally demonstrated when dAM was applied as a wound dressing for the regeneration of the full-thickness urothelial injury.

This is so far the only study that shows the ultrastructure of the superficial urothelial cells on the BFs-enriched dAM scaffolds and even more importantly, the ultrastructure of the superficial urothelial cells of the regenerated urothelia on the dAM wound dressing. In this aspect, we would also like to point out the importance of the ultrastructural analysis in the process of determination of the urothelial differentiation stage. Moreover, based on the ultrastructural characterization of the superficial urothelial cells, we can also assume the functionality of the established urothelial[14,35–37].

Damage of the urothelium can lead to disruption of the blood–urine permeability barrier, permitting the unregulated flow of toxins, ions, and water between the urine and the blood. Rapid resealing of urothelial injuries is thus of great importance for the normal bladder physiology. The majority of the treatments in regenerative urology require reconstruction of the whole urinary tract wall; however, there are urinary tract diseases that particularly affect the urothelium, for example, papillary urinary bladder carcinomas[38]. Such diseases and/or their treatment (i.e., transurethral resection of bladder tumor [TURB]) usually lead to full-thickness injuries of the urothelium. Our results demonstrate that, when used as a wound dressing, the dAM promotes healing of the full-thickness urothelial wound, since it enables the integration of native BFs from the lamina propria into the AM spongy layer and the development of the urothelium from the native urothelial cells which is firmly associated with the dAM basal lamina by hemidesmosomes. Within a week, the nontreated urothelial injuries showed almost no sign of healing. This, however, could also be due to the fact that the control urothelial injuries were not filled with the matrix or another scaffold, as they were in the case of the dAM application.

This study demonstrates the benefits of the AM dressing for the regeneration of the urothelial injury. However, access to the wound and application of such a dressing in the urinary bladder in vivo could be demanding. First, due to the challenges with the introduction of the AM into the bladder and its proper orientation before the application to the wound. And second, due to challenges related to the efficient attachment of the AM graft to the wound. Namely, the urothelium is constantly flushed with urine, and thus the dressing should be properly secured to remain on the place of the injury. In the present study, we applied the AM graft on the urothelial injury with fibrin glue. The fibrin glue contains thrombin and highly concentrated fibrinogen which replicate the final stage of the coagulation cascade when mixed together. Since the fibrin sealant is already broadly used in urological surgery[39] and has proven to be effective in AM transplantation on the ocular surface[40], it could also be useful for the application of the AM dressing in the urinary bladder surgeries (e.g., after TURB). Furthermore, it would be reasonable to also evaluate the forms of the AM which are easier to apply. These include AM homogenate[41,42], AM extracts[43], AM conditioned medium[44], or even amnion-derived cellular cytokine solution[45]. All of these proved to promote the wound-healing process. Moreover, AM homogenate has a potent antimicrobial effect on several clinical uropathogenic strains of *Escherichia coli* strains[42], which is also important for the prevention of postoperative urinary tract infections (UTIs). Therefore, AM dressing or even other AM preparations could be injected into the site of the bladder urothelial injury, where they might accelerate the resealing of the damaged urothelium and prevent UTIs.

Allover, we could hypothesize that AM may be suitable as a dressing of the urothelial injury that occurs during TURB, since it could diminish the possibility of tumor recurrence, by promoting the rapid re-epithelialization of the urothelium. Nevertheless, before considering such an application, the necessary next step should be to evaluate the impact of the AM matrix on attachment, proliferation, and migration of cancer bladder urothelial cells. Since only with this awareness, we could propose a safe and effective treatment.

Conclusions

The present study confirms the suitability of the AM extracellular matrix for the development of differentiated urothelium. We demonstrate that AM allows integration of BFs into its stroma and enables the formation of the differentiated urothelial tissue equivalents in vitro, as well as promotes regeneration of the urothelium when used as a wound dressing. In view of these data and by considering all the precautions required for treating cancerous tissues, the dAM dressing could have a promising potential for use as an implantable device after TURB. The established in vitro models could currently be used as an alternative method for drug testing since only the fully characterized 3D tissue equivalents are suitable to accurately predict the efficacy of newly developed drugs. This is also in accordance with scientifically guiding principles for the more ethical use of animals in testing.

amniotic membranes. This work contributes to the COST Action CA17116 International Network for Translating Research on Perinatal Derivatives into Therapeutic Approaches (SPRINT), supported by COST (European Cooperation in Science and Technology).

Ethical Approval

The use of human amniotic membrane was approved by the National Medical Ethics Committee of Republic of Slovenia.

Statement of Human and Animal Rights

No studies were performed on humans or animals.

Statement of Informed Consent

Written informed consent was obtained from the volunteers for their anonymized information to be published in this article.

Declaration of Conflicting Interests

The author(s) declared no potential conflicts of interest with respect to the research, authorship, and/or publication of this article.

Funding

ORCID iD

Mateja Erdani Kreft https://orcid.org/0000-0001-6486-165X

References

1. Mamede AC, Carvalho MJ, Abrantes AM, Laranjo M, Maia CJ, Botelho MF. Amniotic membrane: from structure and functions to clinical applications. Cell Tissue Res. 2012;349(2): 447–458.

2. Magatti M, Caruso M, De Munari S, Vertua E, De D, Manuelpillai U, Parolini O. Human amniotic membrane-derived mesenchymal and epithelial cells exert different effects on monocyte-derived dendritic cell differentiation and function. Cell Transplant. 2015;24(9):1733–1752.

3. Buhimschi IA, Jabr M, Buhimschi CS, Petkova AP, Weiner CP, Saed GM. The novel antimicrobial peptide beta3-defensin is produced by the amnion: a possible role of the fetal membranes in innate immunity of the amniotic cavity. Am J Obstet Gynecol. 2004;191(5):1678–1687.

4. Lee SB, Li DQ, Tan DT, Meller DC, Tseng SC. Suppression of TGF-beta signaling in both normal conjunctival fibroblasts and pterygial body fibroblasts by amniotic membrane. Curr Eye Res. 2000;20(4):325–334.

5. Lemke A, Ferguson J, Gross K, Penzenstadler C, Bradl M, Mayer RL, Gerner C, Redl H, Wolbank S. Transplantation of human amnion prevents recurring adhesions and ameliorates fibrosis in a rat model of sciatic nerve scarring. Acta Biomater. 2018;66:335–349.

6. Kamiya K, Wang M, Uchida S, Amano S, Oshika T, Sakuragawa N, Hori J. Topical application of culture supernatant from human amniotic epithelial cells suppresses inflammatory reactions in cornea. Exp Eye Res. 2005;80(5):671–679.

7. Ramuta T, Kreft ME. Human amniotic membrane and amniotic membrane-derived cells: how far are we from their use in regenerative and reconstructive urology? Cell Transplant. 2018;27(1):77–92.

8. Koziak A, Salagierski M, Marcheluk A, Szczesniewski R, Sosnowski M. Early experience in reconstruction of long ureteral strictures with allogenic amniotic membrane. Int J Urol. 2007; 14(7):607–610.

9. Adamowicz J, Pokrywczyńska M, Tworkiewicz J, Kowalczyk T, van Breda SV, Tyloch D, Kloskowski T, Bodnar M, Skopinska-Wisniewska J, Marszałek A, Frontczak-Baniewicz M, et al. New amniotic membrane based biocomposite for future application in reconstructive urology. PLoS One. 2016;11(1): e0146012.

10. Barski D, Gerullis H, Ecke T, Yang J, Varga G, Boros M, Pintelon I, Timmermans JP, Otto T. Bladder reconstruction with human amniotic membrane in a xenograft rat model: a preclinical study. Int J Med Sci. 2017;14(4):310–318.

11. Koziak A, Marcheluk A, Dmowski T, Szcześniewski R, Kania P, Dorobek A. Reconstructive surgery of male urethra using human amnion membranes (grafts)–first announcement. Ann Transplant. 2004;9(4):21–24.

12. Romih R, Korosec P, de Mello W, Jezernik K. Differentiation of epithelial cells in the urinary tract. Cell Tissue Res. 2005; 320(2):259–268.

13. Hicks RM. The mammalian urinary bladder: an accommodating organ. Biol Rev Camb Philos Soc. 1975;50(2):215–246.

14. Kreft ME, Hudoklin S, Jezernik K, Romih R. Formation and maintenance of blood-urine barrier in urothelium. Protoplasma. 2010;246(1–4):3–14.

15. Lasič E, Višnjar T, Kreft ME. Properties of the urothelium that establish the blood-urine barrier and their implications for drug delivery. Rev Physiol Biochem Pharmacol. 2015;168:1–29.

16. Baker SC, Shabir S, Southgate J. Biomimetic urothelial tissue models for the in vitro evaluation of barrier physiology and bladder drug efficacy. Mol Pharm. 2014;11(7):1964–1970.

17. Sartoneva R, Haimi S, Miettinen S, Mannerström B, Haaparanta AM, Sándor GK, Kellomäki M, Suuronen R, Lahdes-Vasama T. Comparison of a poly-L-lactide-co-ε-caprolactone and human amniotic membrane for urothelium tissue engineering applications. J R Soc Interface. 2011;8(58):671–677.

18. Sharifiaghdas F, Naji M, Sarhangnejad R, Rajabi-Zeleti S, Mirzadeh H, Zandi M, Saeed M.Comparing supportive properties of poly lactic-co-glycolic acid (PLGA), PLGA/collagen and human amniotic membrane for human urothelial and smooth muscle cells engineering. Urol J. 2014;11(3): 1620–1628.

19. Wang F, Liu T, Yang L, Zhang G, Liu H, Yi X, Yang X, Lin TY, Qin W, Yuan J. Urethral reconstruction with tissue-engineered human amniotic scaffold in rabbit urethral injury models. Med Sci Monit. 2014;20:2430–2438.

20. Sharifiaghdas F, Hamzehiesfahani N, Moghadasali R, Ghaemimanesh F, Baharvand H. Human amniotic membrane as a suitable matrix for growth of mouse urothelial cells in comparison

with human peritoneal and omentum membranes. Urol J. 2007; 4(2):71–78.

21. Jerman UD, Veranič P, Kreft ME. Amniotic membrane scaffolds enable the development of tissue-engineered urothelium with molecular and ultrastructural properties comparable to that of native urothelium. Tissue Eng Part C Methods. 2013; 20(4):317–327.

22. Jerman UD, Kreft ME, Veranič P. Epithelial-mesenchymal interactions in urinary bladder and small intestine and how to apply them in tissue engineering. Tissue Eng Part B Rev. 2015; 21(6):521–530.

23. Yang L, Shirakata Y, Tokumaru S, Xiuju D, Tohyama M, Hanakawa Y, Hirakawa S, Sayama K, Hashimoto K. Living skin equivalents constructed using human amnions as a matrix. J Dermatol Sci. 2009;56(3):188–195.

24. Zupančič D, Mrak Poljšak K, Kreft ME. Co-culturing porcine normal urothelial cells, urinary bladder fibroblasts and smooth muscle cells for tissue engineering research. Cell Biol Int. 2018;42(4):411–424.

25. Jerman UD, Kolenc M, Steyer A, Veranic P, Prijatelj MP, Kreft ME. A novel strain of porcine adenovirus detected in urinary bladder urothelial cell culture. Viruses. 2014;6(6):2505–2518.

26. Višnjar T, Kreft ME. Air-liquid and liquid-liquid interfaces influence the formation of the urothelial permeability barrier in vitro. In Vitro Cell Dev Biol Anim. 2013;49(3):196–204.

27. Kreft ME, Romih R, Sterle M. Antigenic and ultrastructural markers associated with urothelial cytodifferentiation in primary explant outgrowths of mouse bladder. Cell Biol Int. 2002;26(1):63–74.

28. Bouhout S, Goulet F, Bolduc S. A novel and faster method to obtain a differentiated 3-dimensional tissue engineered bladder. J Urol. 2015;194(3):834–841.

29. Langhans SA. Three-dimensional in vitro cell culture models in drug discovery and drug repositioning. Front Pharmacol. 2018;9:6.

30. Nagase H. In: Clendeninn NJ, Appelt K, editors. Matrix metalloproteinase inhibitors in cancer therapy. Humana Press; 2001, p. 39–66.

31. Dietrich-Ntoukas T, Hofmann-Rummelt C, Kruse FE, Schlötzer-Schrehardt U. Comparative analysis of the basement membrane composition of the human limbus epithelium and amniotic membrane epithelium. Cornea. 2012;31(5):564–569.

32. Donjacour AA, Cunha GR. Stromal regulation of epithelial function. Cancer Treat Res. 1991;53:335–364.

33. Chowdhury SR, Aminuddin BS, Ruszymah BH. Effect of supplementation of dermal fibroblasts conditioned medium on expansion of keratinocytes through enhancing attachment. Indian J Exp Biol. 2012;50(5):332–339.

34. Sakai LY, Keene DR, Morris NP, Burgeson RE. Type VII collagen is a major structural component of anchoring fibrils. J Cell Biol. 1986;103(4):1577–1586.

35. Kreft ME, Robenek H. Freeze-fracture replica immunolabelling reveals urothelial plaques in cultured urothelial cells. PLoS One. 2012;7(6):e38509.

36. Zupančič D, Romih R, Robenek H, Žužek Rožman K, Samardžija Z, Kostanjšek R, Kreft ME. Molecular ultrastructure of the urothelial surface: insights from a combination of various microscopic techniques. Microsc Res Tech. 2014; 77(11):896–901.

37. Višnjar T, Kreft ME. The complete functional recovery of chitosan-treated biomimetic hyperplastic and normoplastic urothelial models. Histochem Cell Biol. 2014;143(1):95–107.

38. Babjuk M, Böhle A, Burger M, Capoun O, Cohen D, Compérat EM, Hernández V, Kaasinen E, Palou J, Rouprêt M, van Rhijn BW, et al. EAU guidelines on non-muscle-invasive urothelial carcinoma of the bladder: update 2016. Eur Urol. 2017;71(3): 447–461.

39. Evans LA, Morey AF. Current applications of fibrin sealant in urologic surgery. Int Braz J Urol. 2006;32(2):131–141.

40. Hick S, Demers PE, Brunette I, La C, Mabon M, Duchesne B. Amniotic membrane transplantation and fibrin glue in the management of corneal ulcers and perforations: a review of 33 cases. Cornea. 2005;24(4):369–377.

41. Guo Q, Hao J, Yang Q, Guan L, Ouyang S, Wang J. A comparison of the effectiveness between amniotic membrane homogenate and transplanted amniotic membrane in healing corneal damage in a rabbit model. Acta Ophthalmol. 2011; 89(4):e315–e319.

42. Ramuta T, Starčič Erjavec M, Kreft ME. Amniotic membrane preparation crucially affects its broad-spectrum activity against uropathogenic bacteria. Front Microbiol. 2020;11:469.

43. Kang M, Choi S, Cho Lee AR. Effect of freeze dried bovine amniotic membrane extract on full thickness wound healing. Arch Pharm Res. 2013;36(4):472–478.

44. Kratz G, Haegerstrand A, Palmer B. Growth stimulatory effects of amniotic fluid and amniotic cell conditioned medium on human cells involved in wound healing. Eur J Plast Surg. 1993;16(3):130–133.

45. Franz MG, Payne WG, Xing L, Naidu DK, Salas RE, Marshall VS, Trumpower CJ, Smith CA, Steed DL, Robson MC. The use of amnion-derived cellular cytokine solution to improve healing in acute and chronic wound models. Eplasty. 2008;8:e21.